Contents of Endometriotic Cysts, Especially the High Concentration of Free Iron, Are a Possible Cause of Carcinogenesis in the Cysts through the Iron-Induced Persistent Oxidative Stress

Ken Yamaguchi,[1] Masaki Mandai,[1] Shinya Toyokuni,[2] Junzo Hamanishi,[1] Toshihiro Higuchi,[1] Kenji Takakura,[1] and Shingo Fujii[1,3]

Abstract

Purpose: Endometriotic cysts are known to transform into ovarian cancers, such as clear cell and endometrioid carcinomas. We hypothesized that an iron-rich environment produced by the repetition of hemorrhage in the endometriotic cysts during the reproductive period may play a crucial role in carcinogenesis in the cysts through the iron-induced persistent oxidative stress.

Experimental Design: Contents of human ovarian cysts, including 21 endometriotic cysts, 4 clear cell carcinomas, and 11 nonendometriotic cysts, were analyzed for the concentrations of free "catalytic" iron, lactose dehydrogenase, potential antioxidant, lipid peroxide, and 8-hydroxy-2′-deoxyguanosine (8-OHdG). Iron deposition and 8-OHdG levels were also analyzed histologically. Reactive oxygen species and the mutagenicity of the contents in endometriotic cyst were determined *in vitro*.

Results: The concentration of free iron in endometriotic cysts (100.9 mmol/L) was significantly higher than that in nonendometriotic cysts (0.075 mmol/L; $P < 0.01$). The average concentrations of lactose dehydrogenase, potential antioxidant, lipid peroxide, and 8-OHdG were also significantly higher in endometriotic cysts ($P < 0.01$). There was a correlation between the concentration of free iron and that of 8-OHdG ($P < 0.01$). Histologically, we could observe iron deposits more abundantly in endometriotic cysts than in nonendometriotic cysts ($P < 0.01$). The level of 8-OHdG in carcinoma associated with endometriosis was higher than that of carcinoma without endometriosis ($P < 0.05$). *In vitro* analyses showed that the contents of endometriotic cyst could produce more reactive oxygen species and could induce gene mutations more frequently than the contents in the other cysts.

Conclusions: Abundant free iron in the contents of endometriotic cysts was strongly associated with greater oxidative stress and frequent DNA mutations. A long-standing history of the RBCs accumulated in the ovarian endometriotic cysts during the reproductive period produces oxidative stress that is a possible cause for the malignant change of the endometriotic cyst.

Endometriosis is a common benign gynecologic disorder characterized by the presence of uterine endometrial tissue, such as endometrial glandular epithelium and stroma, outside the normal location (1). Endometriotic cyst is an ovarian endometriosis that contains chocolate-like fluid as the result of accumulation of menstruation-like hemorrhagic blood in the cyst during the reproductive period. It is well known that ovarian cancer arises in the endometriotic cysts (2, 3). However, the mechanism of malignant change of the endometriosis in the endometriotic cyst is not yet elucidated.

Several epidemiologic studies have suggested the association of endometriosis and ovarian cancer (2–5), showing the high risk of ovarian cancer in women with a long-standing history (>10 years) of ovarian endometriosis (6). Pathologically atypical endometriosis, which is characterized by endometriotic glands with cytologic and/or architectural atypia (7), was reported in 22.6% (7 of 31) of endometrioid and 36.0% (18 of 50) of clear cell adenocarcinomas of the ovary, whereas in only 1.7% (4 of 255) of cases of ordinal ovarian endometriosis (8). Ovarian cancer arisen in the endometriotic cyst shows the predominant incidence of clear cell and endometrioid types (>40%), whereas serous and mucinous adenocarcinoma is predominant in ovarian cancers unrelated to endometriosis (8), suggesting the different mechanism of carcinogenesis between the cancer in ovarian endometriotic cyst and ovarian cancer in general.

Bimolecular features of ovarian cancers arisen in the endometriotic cyst have also been studied extensively, such as mutation of the *K-RAS* and *PTEN* genes (9), alteration of *BCL-2* and P53 (10), decreased expression of hMLH and PTEN (11), and increased vascular endothelial growth factor (12). Loss of heterozygosity in the oncosuppressor region in endometriosis (7, 13) and the common loss of heterozygosity in concomitant

Authors' Affiliations: Departments of [1]Gynecology and Obstetrics and [2]Pathology and Biology of Diseases, Graduate School of Medicine, Kyoto University; and [3]National Hospital Organization Kyoto Medical Center, Kyoto, Japan

Received 7/2/07; revised 9/5/07; accepted 10/9/07.

The costs of publication of this article were defrayed in part by the payment of page charges. This article must therefore be hereby marked *advertisement* in accordance with 18 U.S.C. Section 1734 solely to indicate this fact.

Requests for reprints: Shingo Fujii, Department of Gynecology and Obstetrics, Graduate School of Medicine, Kyoto University, 54 Kawahara-cho Shogoin, Sakyo-ku, Kyoto 606-8507, Japan. Phone: 81-75-751-3269; Fax: 81-75-761-3967; E-mail: sfu@kuhp.kyoto-u.ac.jp.

©2008 American Association for Cancer Research.

doi:10.1158/1078-0432.CCR-07-1614

Downloaded from http://aacrjournals.org/clincancerres/article-pdf/14/1/32/1974769/32.pdf by guest on 04 August 2024

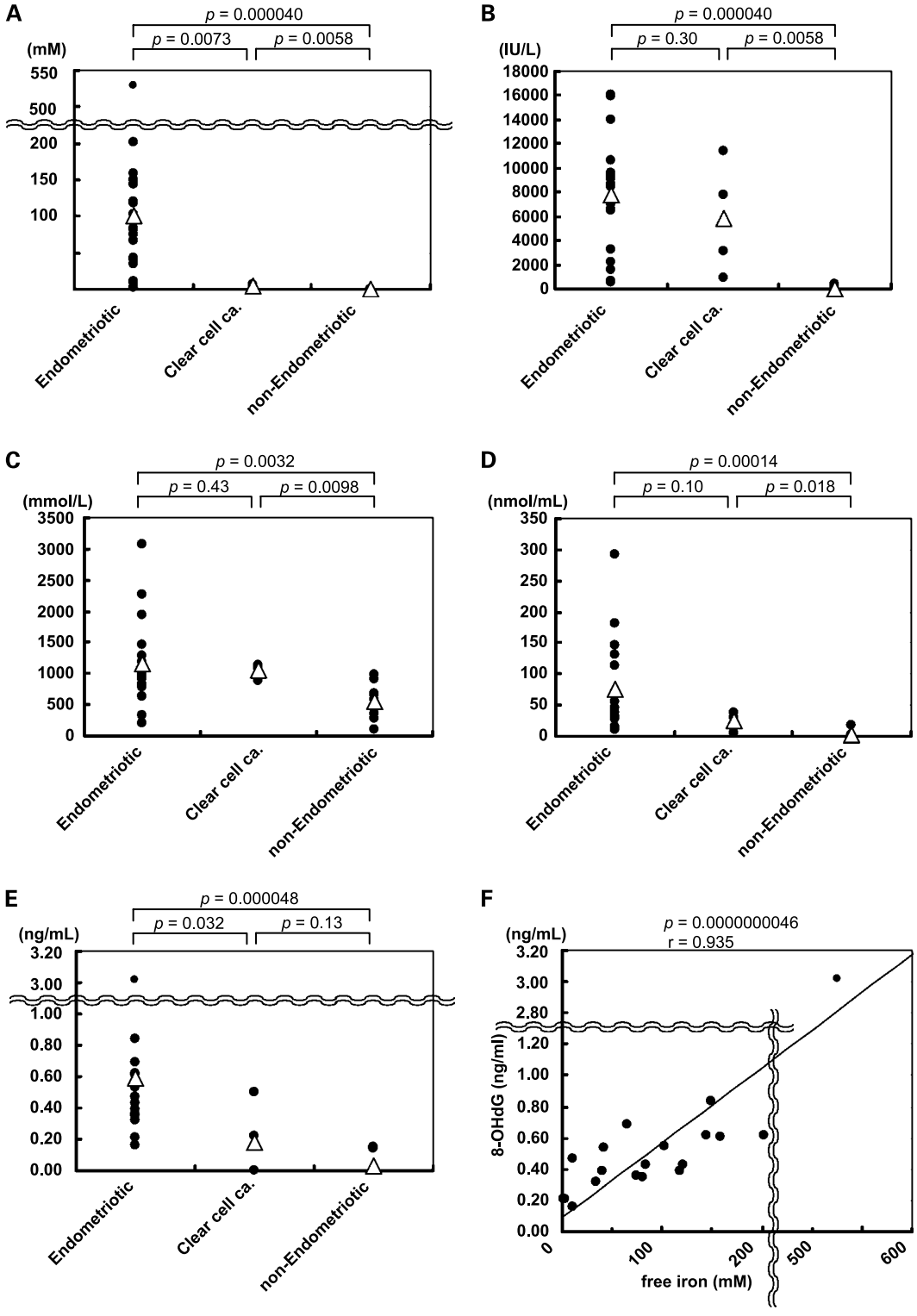

Fig. 1. *A,* concentration of free iron in endometriotic cysts (n = 21; mean ± SD: 100.9 ± 115.1 mmol/L), clear cell carcinoma (n = 4; mean ± SD: 4.27 ± 2.42 mmol/L), and nonendometriotic cysts (n = 11; mean ± SD: 0.075 ± 0.081 mmol/L). *B,* concentration of lactose dehydrogenase as a tissue damage marker in endometriotic cysts (n = 20; 7,715 ± 4,540 IU/L), clear cell carcinoma (n = 4; 5,817 ± 4,739 IU/L), and nonendometriotic cysts (n = 11; 64.5 ± 102.5 IU/L). *C,* concentration of PAO as an antioxidant marker in endometriotic cysts (n = 18; 1,164 ± 687 mmol/L), clear cell carcinoma (n = 4; 1,062 ± 119 mmol/L), and nonendometriotic cysts (n = 11; 557 ± 264 mmol/L). *D,* concentration of LPO as an oxidative marker in endometriotic cysts (n = 18; 75.7 ± 73.4 nmol/mL), clear cell carcinoma (n = 3; 25.2 ± 17.7 nmol/mL), and nonendometriotic cysts (n = 10; 2.93 ± 5.48 nmol/mL). *E,* concentration of 8-OHdG as an oxidative and DNA damage marker in endometriotic cysts (n = 19; 0.588 ± 0.612 ng/mL), clear cell carcinoma (n = 4; 0.181 ± 0.237 ng/mL), and nonendometriotic cysts (n = 11; 0.0266 ± 0.0592 ng/mL). *F,* a significant positive correlation was found between free iron and 8-OHdG (P = 0.0000000046). Δ, mean; ●, each result.

Downloaded from http://aacrjournals.org/clincancerres/article-pdf/14/1/32/1974769/32.pdf by guest on 04 August 2024

endometriosis and carcinoma (14) are also reported. The genetic mouse model of peritoneal endometriosis is reported to develop by the induction of oncogenic *K-ras* and endometrioid ovarian adenocarcinoma by further deletion of *Pten* (15). Therefore, several molecular mechanisms involved in the carcinogenesis of endometriosis have been identified. However, the precise mechanism that can explain the uniqueness of carcinogenesis in the endometriotic cyst still remains to be elucidated.

Repeated hemorrhage into the cyst during the menstrual cycle and the accumulation of blood components in the cyst are characterized in the endometriotic cyst. In this study, we focused on the contents of endometriotic cysts, especially the high concentration of free iron, as the cause of carcinogenesis of the cyst. Under the hypothesis that the fluid of endometriotic cysts containing iron contributes to genetic changes via oxidative stress (16–18) and may be one of the major causes of the malignant transformation of endometriotic cysts, we examined the concentration of iron in the endometriotic cyst and other cysts. As well, we examined the products of oxidative stress in the contents of the cysts. *In vitro* experiments were done whether the contents of endometriotic cysts can induce DNA damage or not.

Materials and Methods

Samples. Samples were obtained from patients with ovarian cysts treated surgically at Kyoto University Hospital with written forms of consent. The contents of the ovarian cysts were stored at -80°C immediately after surgery or centrifuged at 3,000 or 4,000 rpm for 10 min; the supernatants were then stored at -80°C.

Cell culture. Immortalized ovarian surface epithelial cells established by us were maintained as described previously (19, 20). Human immortalized endometrial glandular cells, kindly provided by Dr. S. Kyo (Kanazawa University, Kanazawa, Japan; ref. 21), and Chinese hamster lung fibroblast cell line (V79 cells) purchased from RIKEN BioResource Center Cell Bank, were cultured in DMEM (Nikken Bio Medical Laboratory) containing penicillin-streptomycin (100 units/mL penicillin, 100 μg/mL streptomycin; Nacalai Tesque) and 10% fetal bovine serum (v/v; BioWest).

Detection of free iron (iron ions) in cyst fluid. The reaction mixture was added to plastic metal ion–free disposable tubes in the following order: 0.5 mL of calf thymus DNA sodium salt type I (1 mg/mL; Sigma-Aldrich), 0.05 mL bleomycin hydrochloride (1 mg/mL; kindly provided by Nippon Kayaku), 0.1 mL $MgCl_2$ (50 mmol/L; Nacalai Tesque), 0.1 mL of sample, 0.05 mL HCl (10 mmol/L; Nacalai Tesque), 0.1 mL of ultrapure water, and 0.1 mL of 0.14% ascorbic acid solution (w/v; Nacalai Tesque). A standard curve was prepared using $Fe(NO_3)_3$ dissolved in ultrapure water. The samples of endometriotic cyst fluids were dissolved in ultrapure water at 1- to 40,000-fold to obtain concentrations of free iron between 0 and 250 μmol/L. The tube contents were mixed before and after addition of ascorbate and then incubated at 37°C for 2 h with shaking. Then, 1 mL of 0.1 mol/L EDTA (Dojindo) was added to stop the reaction, and the tube contents were mixed with 1 mL of 1% thiobarbituric acid (w/v; Merck) in 50 mmol/L NaOH (Nacalai Tesque) and 1 mL of 25% HCl (v/v; Nacalai Tesque). The solutions were heated at 100°C for 15 min and cooled, and the chromogen was measured by the absorbance at 532 nm.

Detection of lactose dehydrogenase in cyst fluid. Stored samples for chemical analysis were thawed and centrifuged at 3,000 rpm for 10 min and analyzed by the method recommended by the Japan Society of Clinical Chemistry using CicaLiquid lactose dehydrogenase J (Kanto Chemical Co., Inc.). If the result was >1,000 IU/L, the sample was diluted 10-fold in 0.9% NaCl solution.

Detection of potential antioxidant in cyst fluid. Potential antioxidant (PAO) was measured using a PAO assay kit (Japan Institute for the Control of Aging, Nikken SEIL Corp.), which measures antioxidant capacity using the reduction of cupric ion (Cu^{2+} to Cu^{+}), according to the manufacturer's protocol. Stored samples were thawed and centrifuged at 10,000 × *g* at 4°C for 60 min. Supernatants ultrafiltered with a cutoff molecular weight of 10,000 were analyzed using the kit.

Detection of lipid peroxide in cyst fluid. Stored samples for chemical analysis were thawed and centrifuged at 3,000 rpm for 10 min, and lipid peroxide (LPO) levels were determined by the hemoglobin-methylene blue method using Determiner LPO (Kyowa Medix Co. Ltd.).

Detection of 8-hydroxy-2-deoxyguanosine in cyst fluid. 8-hydroxy-2′-deoxyguanosine (8-OhdG) is one of the major oxidatively modified DNA base products *in vivo* and is mutation prone (G:C to T:A transversion; ref. 22). Stored samples were thawed and centrifuged at 10,000 × *g* at 4°C for 60 min. Supernatants ultrafiltered with a cutoff molecular weight of 10,000 were analyzed using a High-Sensitive 8-OHdG Check ELISA kit (Japan Institute for the Control of Aging, Nikken SEIL Corp.).

Prussian blue staining of human tissue samples for iron detection. Tissues were fixed in 10% buffered formalin and embedded in paraffin. Sections were deparaffinized and immersed for 20 min in a working solution consisting of equal amounts of 5% potassium ferrocyanide [$K_4Fe(CN)_6$] and 5% hydrochloric acid solution (Nacalai Tesque). Counterstaining was done with Nuclear Fast Red (Lab Vision Corp.) for 5 min.

Evaluation of iron deposits in human tissue samples. Iron deposition was graded after Prussian blue staining according to the method of Blanc et al. (23), with some modifications, as follows: grade 0, absence of iron; grade 1, mild deposition with iron barely confirmed at ×400 magnification; grade 2, moderate deposition with iron visible at ×40 magnification; and grade 3, severe deposition with iron visible on glass slides to the naked eye.

Immunohistochemical analysis of 8-OHdG in human tissue samples. Tissues fixed in 10% buffered formalin and embedded in paraffin were deparaffinized and hydrated, and immunohistochemical staining of 8-OHdG was done as described previously (24) using monoclonal anti-8-OHdG antibody (N45.1) as the primary antibody, biotin-labeled rabbit anti-mouse IgG antibody as the secondary antibody, and peroxidase-conjugated streptavidin (Vector Laboratories).

Evaluation of 8-OHdG in human tissue samples. The formation of 8-OHdG was evaluated by an immunohistochemical method and defined as follows: ++, obviously stronger than normal ovarian stroma; +, slightly or partially (<10%) stronger than normal ovarian stroma; and -, equivalent to normal ovarian stroma. Evaluation was done by two independent pathologists who had no knowledge of the clinical information.

In vitro ***intracellular reactive oxygen species detection assay.*** Intracellular reactive oxygen species (ROS) were detected *in vitro* as described previously using 2′,7′-dichlorodihydrofluorescein diacetate (25, 26). Human immortalized ovarian surface epithelial cells and human immortalized endometrial glandular cells were plated onto 12-well plates at 50% to 60% confluence. On the next day, the cells were gently washed with PBS and incubated with the contents of various cysts (at a dilution of 1:5) or ferric nitrilotriacetate (Fe-NTA) for 2 h. Fe-NTA, an iron chelate, was prepared as described previously (27). Then, the cells were washed and incubated with 5 μmol/L 2′,7′-dichlorodihydrofluorescein diacetate (Sigma-Aldrich) for 30 min at room temperature. After that, the cells were rinsed and harvested for flow cytometry analysis. In each analysis, at least 20,000 living cells were used to measure intracellular green fluorescence with excitation at 488 nm and emission at 525 nm by FACSCalibur flow cytometry (Becton Dickinson). Each group contained four independent samples.

In vitro ***DNA damage detection assay (V79/hypoxanthine guanine phosphoribosyltransferase gene mutation assay).*** Hypoxanthine guanine

Downloaded from http://aacrjournals.org/clincancerres/article-pdf/14/1/32/1974769/32.pdf by guest on 04 August 2024

Table 1. Prussian blue staining of iron deposits in ovarian tumors

Iron deposits (grade 0-3)	0	1	2	3	P
Endometriotic cysts (n = 20)	2	0	4	14	*
Nonendometriotic cysts (n = 14)	13	1	0	0	**
Ovarian cancer with endometriosis (n = 20)	3	6	9	2	
Ovarian cancer without endometriosis (n = 12)	8	1	2	1	

NOTE: A significant difference (P = 0.00013) was found between endometriotic cysts (*) and nonendometriotic cysts (**).

phosphoribosyltransferase (HGPRT) is an enzyme essential for the salvage pathway of DNA synthesis. Normal mammalian cells expressing HGPRT cannot survive in medium containing 6-thioguanine (6-TG) because HGPRT converts 6-TG into a cytotoxic metabolite that is incorporated into host DNA and results in inhibition of further DNA synthesis. In contrast, HGPRT-mutated mammalian cells can survive and proliferate in 6-TG–containing medium. Hence, the mutagenic activity of specific substances can be evaluated by counting 6-TG–resistant colonies (28), with some modifications. Briefly, V79 cells were preselected in the medium containing hypoxanthine, aminopterin, and thymidine (Mediatech, Inc.) and plated onto six-well plates at 2×10^6 per well. After 24 h of incubation, the medium was exchanged for medium containing the test materials and the cultures were further incubated for 24 h. Then, the cells were rinsed with PBS and harvested, plated onto 100-mm culture dishes at 1×10^6 per dish, and cultured for 6 days, harvested, replated in 6-TG–containing medium (10 μg/mL; Sigma-Aldrich) at 3×10^6 per 100-mm dish, and cultured for another 12 days. Each treatment was done in triplicate using three samples in each experiment. The colonies were stained with Giemsa's solution (Nacalai Tesque), and the number of colonies in each dish was counted. Ethyl methanesulfonate (Nacalai Tesque; 500 μg/mL) was used as a positive control and normal medium was used as a negative control.

Statistics. All data are expressed as mean ± SD. Analysis of the constituents of the ovarian cyst contents (free iron, lactose dehydrogenase, PAO, LPO, and 8-OHdG) and the data from *in vitro* studies was done using the Kruskal-Wallis H test. Comparisons between two groups were done using the Mann-Whitney U test with Bonferroni correction. The correlation between 8-OHdG and free iron was evaluated by Spearman's correlation. Comparison between observed frequency and expected frequency between 8-OHdG and iron deposition and correlation of 8-OHdG and iron deposits were done by an m × n χ^2 test and Fisher's test, and Yates' m × n χ^2 test, respectively. $P < 0.05$ was considered statistically significant.

Results

Detection of free iron (iron ions) in endometriotic and nonendometriotic cyst contents. The average concentration of free iron in endometriotic cysts (mean ± SD: 100.9 ± 115.1 mmol/L) was higher than that in nonendometriotic benign cysts (0.075 ± 0.081 mmol/L; P = 0.000040; Fig. 1A). Free iron concentrations in clear cell carcinomas (4.27 ± 2.42 mmol/L) were lower than in endometriotic cysts (P = 0.0073) but higher than in nonendometriotic benign cysts (P = 0.0058).

Detection of oxidative stress–related factors in cyst contents. The lactose dehydrogenase level, a tissue damage marker, was significantly higher in endometriotic cysts (7,715 ± 4,540 IU/L) than in the other ovarian benign cysts (64.5 ± 102.5 IU/L; P = 0.000040). The average concentration of PAO, an antioxidant marker, was significantly higher in endometriotic cysts (1,164 ± 687 mmol/L) than that in serous or mucinous cystadenoma (557 ± 264 mmol/L; P = 0.0032). The concentrations of LPO, an oxidative marker, and 8-OHdG, an oxidative DNA damage marker, were significantly higher in endometriotic cysts (75.7 ± 73.4 nmol/mL and 0.588 ± 0.612 ng/mL, respectively) than those in the other cysts (2.93 ± 5.48 nmol/mL, P = 0.00014, and 0.0266 ± 0.0592 ng/mL, P = 0.000048, respectively; Fig. 1B-E). Clear cell carcinoma showed intermediate levels between endometriotic cysts and other benign cysts with regard to all the substances. The concentration of 8-OHdG was significantly correlated with that of free iron (P = 0.0000000046; Fig. 1F).

Iron deposits in ovarian cysts and ovarian cancer tissues. Iron deposition in endometriotic epithelial cells was observed histologically by Prussian blue staining (Table 1). In endometriotic cysts, grade 3 was scored in 14 cases (70%), whereas in other benign ovarian cysts, grade 0 was scored in all cases but one (92.9%). In endometriotic cysts, iron deposits were detected in the stroma and sometimes in epithelial glandular cells (Fig. 2A and B). There was a statistically significant difference in iron deposition between endometriotic cysts and nonendometriotic cysts (P = 0.00013). In ovarian cancer without endometriotic cysts, grade 0 was scored in eight cases (66.7%). In ovarian cancer with endometriotic cysts, grade 0 was scored in three cases (15%), grade 1 in six cases (30%), grade 2 in nine cases (45%), and grade 3 in two cases (10%). Several clear cell cancers with endometriosis showed iron deposits, especially in the transformation area between endometriosis and ovarian cancer cells (Fig. 2C), whereas only one malignant case without endometriosis contained grade 3 iron deposition. Atypical endometriosis was observed in the transformation area of five clear cell cancer cases. Four cases of them showed grade 2 iron deposition in the stromal area but not in the epithelium (Fig. 2D).

Oxidative DNA damage by iron in ovarian tissues. Immunohistochemically 8-OHdG was positive in glands in endometriotic cysts (Fig. 3A) and in ovarian cancer cells accompanied by endometriosis (Fig. 3B). Epithelia of atypical endometriosis were also stained positively. Ovarian cancers without endometriosis showed a similar intensity to normal tissue (Fig. 3C and D). The 8-OHdG levels are summarized in Table 2. Ovarian cancers accompanied by endometriosis showed significantly stronger staining of 8-OHdG than those without endometriosis (P = 0.013). Histopathologic analysis showed a significant correlation between iron deposition and 8-OHdG (P = 0.047).

In vitro *intracellular ROS detection assay.* Fe-NTA was used as iron in the "free" form. Each cyst type included four samples (the average concentrations of free iron in endometriotic cysts, serous cystadenomas, and mucinous cystadenomas were 59.5 ± 46.9 mmol/L, 0.091 ± 0.11 mmol/L, and 0.080 ± 0.086 mmol/L, respectively). Both the immortalized endometrial glandular cells (Fig. 4A) and the immortalized ovarian surface epithelial cells (Fig. 4B) produced significantly higher levels of ROS when treated with the contents of endometriotic cyst and with Fe-NTA than on treatment with other cystadenomas ($P < 0.05$). Dose dependency was observed in the Fe-NTA study ($P < 0.05$; data not shown).

In vitro *DNA damage detection (V79/HGPRT gene mutation assay).* Fe-NTA produced mutations with dose dependency,

Downloaded from http://aacrjournals.org/clincancerres/article-pdf/14/1/32/1974769/32.pdf by guest on 04 August 2024

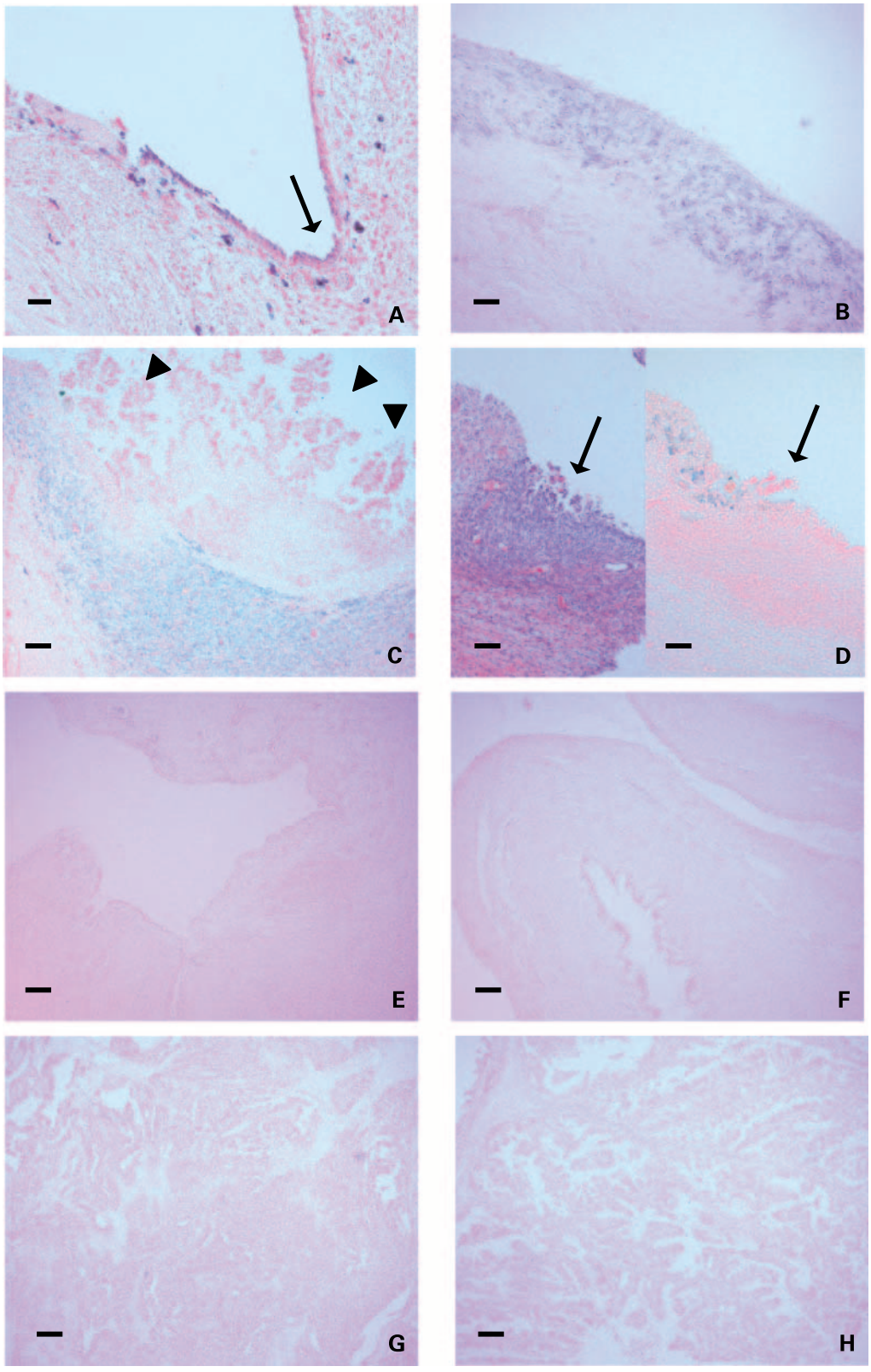

Fig. 2. Prussian blue staining of iron deposition in ovarian tumors. Iron deposits were detected in glandular endometrium (*A, arrow*) and in the stroma (*B*) of endometriotic cysts but not in serous cystadenoma (*E*) or mucinous cystadenoma (*F*). Iron deposits were detected in the stroma beneath clear cell carcinoma adjacent to an endometriotic lesion (*C, arrowheads*), but they were not observed in serous (*G*) or mucinous (*H*) adenocarcinomas. Atypical endometriosis with grade 2 iron deposition was observed in the transformation area of clear cell cancer cases. *D,* left, H&E staining; right, Prussian blue staining. Arrows, epithelium. Bars, 1 mm (*B-H*) and 100 μm (*A*).

Downloaded from http://aacrjournals.org/clincancerres/article-pdf/14/1/32/1974769/32.pdf by guest on 04 August 2024

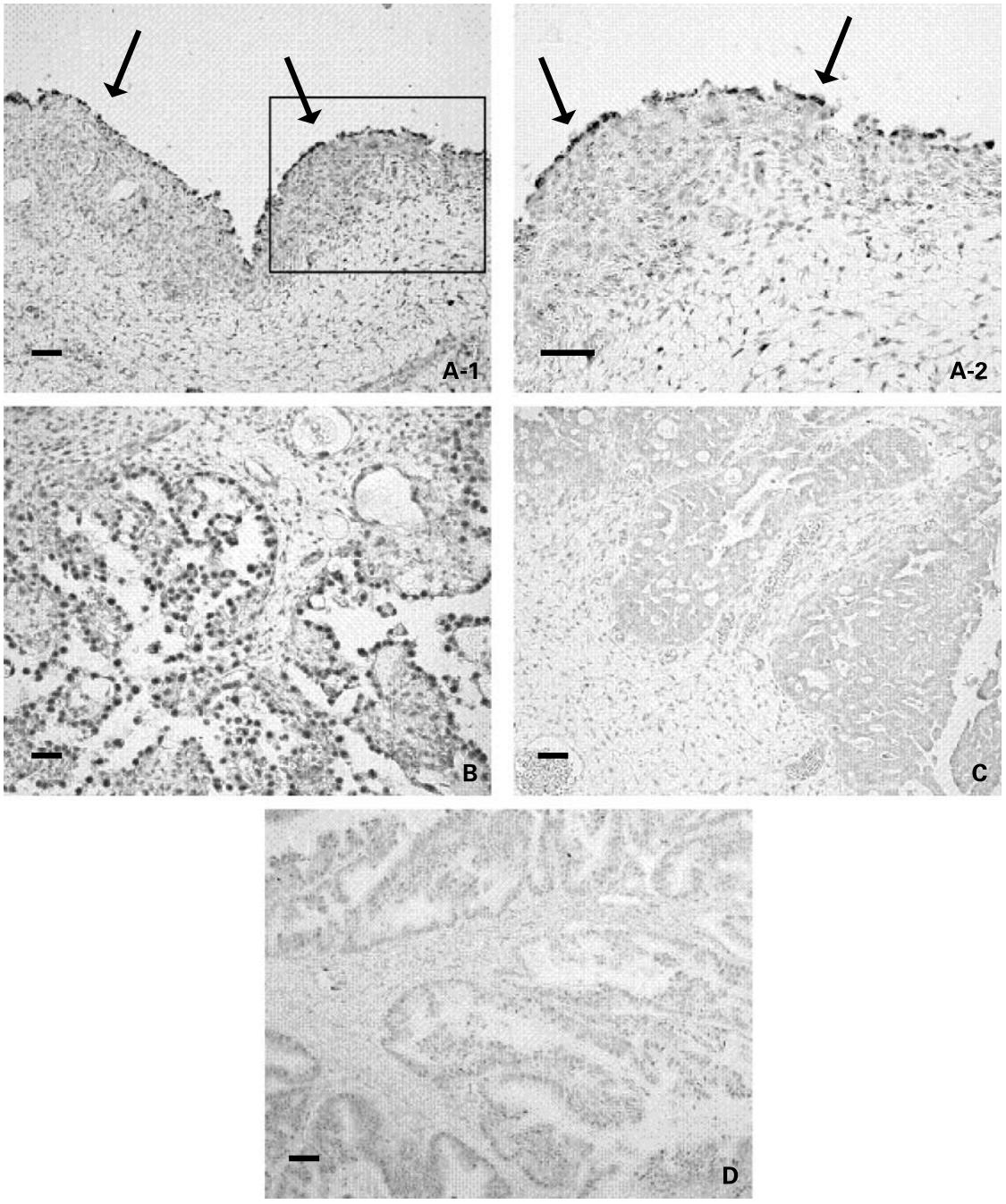

Fig. 3. Immunohistochemical analysis of 8-OHdG in ovarian tumors. *A,* intense 8-OHdG formation was observed in endometriotic glandular epithelial cells (*arrows*) along with faint expression in endometrial stroma. Cases of clear cell carcinoma accompanied by endometriosis showed strong formation of 8-OHdG (*B*), whereas most of the ovarian cancers without endometriosis showed similar level to normal ovarian stroma (*C*, serous adenocarcinoma; *D*, mucinous adenocarcinoma). Bar, 100 μm.

especially at >1,000 μmol/L on V79 cells (data not shown). The concentrations of free iron were 10.6 and 40.7 mmol/L in endometriotic cysts, 0.424 mmol/L in serous cystadenomas, and 0.454 mmol/L in mucinous cystadenomas. The contents of endometriotic cyst showed a significantly higher frequency of mutation than the contents of serous or mucinous cystadenoma ($P < 0.05$; Fig. 4C).

Discussion

The analysis of the contents of various ovarian cysts revealed that endometriotic cyst has extraordinarily high concentration of iron compared with the normal serum and the contents of the other ovarian cysts. This seems natural considering that the fluid in endometriotic cysts is the result of repeated hemorrhage.

Downloaded from http://aacrjournals.org/clincancerres/article-pdf/14/1/32/1974769/32.pdf by guest on 04 August 2024

Table 2. Immunohistochemical analysis of 8-OHdG in ovarian tumors

8-OHdG	-	+	++	P
Endometriotic cysts (n = 20)	0	3	17	
Ovarian cancer with endometriosis (n = 20)	2	2	16	*
Ovarian cancer without endometriosis (n = 12)	6	4	2	**

NOTE: A significant difference (P = 0.013) was found between ovarian cancers with (*) and without (**) endometriosis.

Iron is an essential metal in physiologic function; however, the free or "catalytic" form of iron mediates the production of ROS via the Fenton reaction and induces oxidative stress (16–18). ROS in biological systems induce oxidative stress and lead to iron-induced carcinogenesis (17). In humans, dietary iron is thought to be a risk for gastrointestinal cancers (29, 30) and increased body iron stores are reported to associate with poor prognosis of several human malignant neoplasms (31–34). Moreover, patients with genetic hemochromatosis had ~200 times greater risk for primary hepatocellular carcinoma than the age-matched control population (35–37). Therapeutic iron reduction (phlebotomy and low iron diet) decreased the hepatic 8-OHdG levels and the risk of hepatocellular carcinoma development in patients with chronic hepatitis C virus (38). In animal studies, repeated i.m. injections of iron-dextran complex caused sarcoma in rats (39) as well Fe-NTA renal cell carcinoma in rats (40, 41) and ferric saccharate mesothelioma in mice (42). An iron-enriched diet significantly increased the incidence of colorectal tumors in a mouse ulcerative colitis model (43). Thus, iron induces carcinogenesis in many organs and several reports have indicated the role of iron in the pathogenesis of endometriosis (44, 45), but as far as we know, there is no report suggesting the role of iron in carcinogenesis from endometriotic cysts.

Many *in vitro* and *in vivo* experimental data show that oxygen free radicals generated by free iron induce DNA damage and mutation (46). In this study, the average concentration of free iron in endometriotic cysts exceeded 100 mmol/L (100 μmol/g), which is comparable with reported iron concentration in hepatic carcinoma tissue (3-100 μmol/g dry weight; refs. 23, 47). Prussian blue staining revealed iron deposits in the stroma and endometrial glandular cells of endometriotic cysts (Fig. 2; Table 1). Increased iron deposition has been reported to be associated with hepatocellular carcinoma (48) with high iron concentrations in noncancerous tissue adjacent to the cancer (47) and iron deposits in nontumoral liver (49), suggesting that iron accumulation in normal tissue precedes malignant transformation. The data in the endometriotic cyst are similar to those of in hepatocellular carcinoma that is sufficient amount of iron to induce malignant transformation. Because there was no case of atypical endometriosis without carcinoma, we could not evaluate the contents of atypical endometriosis that is considered as the precancerous lesion in the endometriotic cysts. However, at least we could confirm iron deposition in the areas of atypical endometriosis that was observed adjacent to clear cell carcinoma (Fig. 2D).

We further evaluated the oxidation-reduction status of endometriotic cysts. The level of lactose dehydrogenase, which

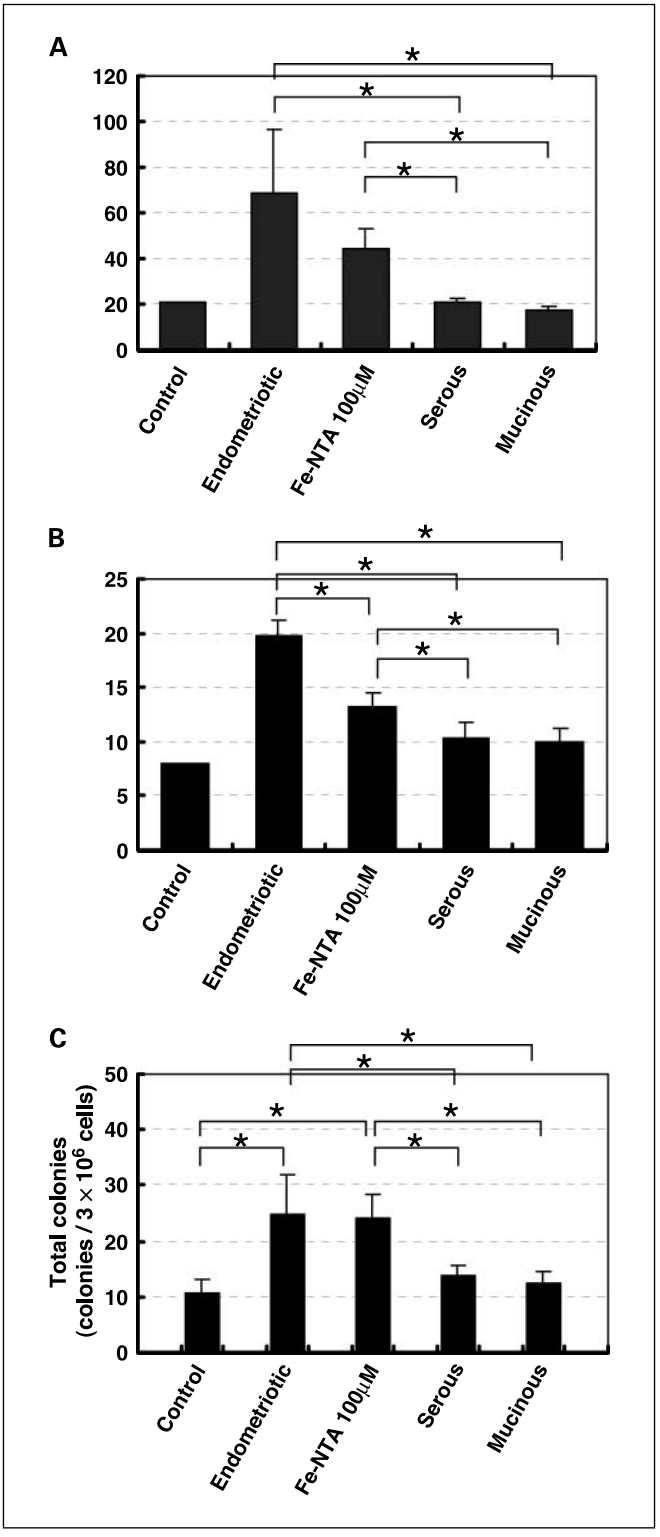

Fig. 4. Generation of ROS in immortalized endometrial glandular cells (*A*) and in immortalized ovarian surface epithelial cells (*B*). The cells were cultured with Fe-NTA (100 μM) and the contents of endometriotic cysts, serous cystadenoma, and mucinous cystadenoma and ROS were detected by measuring 2′,7′-dichlorodihydrofluorescein diacetate. The contents of endometriotic cyst and Fe-NTA generated significantly more ROS than the contents of serous or mucinous cystadenoma ($P < 0.05$). *C,* DNA mutation was detected by counting 6-TG – resistant colonies of V79 cells. Mutations were more frequently induced by Fe-NTA and endometriotic cyst fluid than by the contents of serous or mucinous cystadenoma ($P < 0.05$). *, $P < 0.05$.

Downloaded from http://aacrjournals.org/clincancerres/article-pdf/14/1/32/1974769/32.pdf by guest on 04 August 2024

indicates cellular and tissue damage, was significantly higher in endometriotic cysts than in other benign ovarian cysts (Fig. 1B). The levels of LPO, which indicates lipid peroxidation, 8-OhdG, which indicates oxidative DNA damage, and PAO, which represents antioxidant capacity, were also higher in endometriotic cysts (Fig. 1C-E). These data indicate that endometriotic cysts are exposed to greater oxidative stress and that antioxidation activity is also higher. It is of note that there was a strong positive correlation between the concentration (Fig. 1F) and localization (Figs. 2 and 3; Tables 1 and 2) of 8-OHdG and those of free iron, suggesting that iron facilitates oxidative DNA damage that relates carcinogenesis in humans (38).

The potentiality of endometriotic cyst contents examined using immortalized epithelial cells for the induction of oxidative stress and DNA mutations revealed that cells treated with endometriotic fluid showed higher levels of ROS (Fig. 4A and B) and more frequent V79/HGPRT gene mutation (Fig. 4C) than those treated with the other cystic contents. These data indicate that the fluid in endometriotic cysts can induce oxidative stress and DNA mutation in viable cells. It was, however, difficult to detect the HGPRT gene mutation when we used immortalized ovarian and endometrial epithelial cells instead of V79 cells, which is highly susceptible to mutation. This implies that gene mutation under physiologic conditions may occur more infrequently and that the actual occurrence of carcinoma takes a long time.

In summary, the results shown here indicate that endometriotic cysts contain significantly more iron than other ovarian cysts and iron deposits in endometriotic tissues. Measurement of biochemical markers suggests that the environment inside endometriotic cysts is affected by severe oxidative stress, and the glandular epithelium in endometriotic cysts contains more severe oxidative DNA damage compared with other cysts. The constituents of endometriotic cysts can induce oxidative stress and DNA damage in cultured cells *in vitro*. These data collectively suggest that the contents of endometriotic cysts, especially free iron, play a crucial role in the carcinogenesis from endometriosis, and this may explain the uniqueness of carcinogenesis from endometriosis.

The cyst contents of carcinoma accompanied by endometriosis also had a high concentration of iron, presumably reflecting the nature of the precursor lesion, an endometriotic cyst. However, it was lower than that of endometriotic fluid. The reason for this is unclear, but the most likely explanation is that the contents of the cysts were diluted after the development of carcinoma due to rapid production of fluid by the cancer cells, as rapid growth of the mass is often seen after malignant transformation. Therefore, clinically, high-risk cases may be detected by evaluating the concentration of iron in the cyst with magnetic resonance imaging and surgical removal of the cyst may have an advantage over observation in terms of prevention of cancer. It is, however, important to note that the results here do not provide evidence that iron is solely the cause of carcinogenesis; other factors such as cytokines specifically produced by endometriotic cells may also contribute to oxidative damage.

Interestingly, cancers accompanied by endometriosis showed relatively strong 8-OHdG staining compared with other types of cancer, suggesting that they survive under high oxidative stress. Although the number of observed cases was small, we also found iron deposition as well as 8-OHdG staining in the area of atypical endometriosis. Clinically, clear cell carcinoma has unique characteristics, such as relatively slow growth and chemoresistance, compared with typical ovarian cancers that are not accompanied by endometriosis. Clear cell carcinoma might acquire these characters in the carcinogenic process in the environment under persistent oxidative stress (22).

References

1. Giudice LC, Kao LC. Endometriosis [review]. Lancet 2004;364:1789–99.
2. Somigliana E, Vigano' P, Parazzini F, Stoppelli S, Giambattista E, Vercellini P. Association between endometriosis and cancer: a comprehensive review and a critical analysis of clinical and epidemiological evidence [review]. Gynecol Oncol 2006;101:331–41.
3. Kobayashi H, Sumimoto K, Moniwa N, et al. Risk of developing ovarian cancer among women with ovarian endometrioma: a cohort study in Shizuoka, Japan. Int J Gynecol Cancer 2007;17:37–43.
4. Mostoufizadeh M, Scully RE. Malignant tumors arising in endometriosis. Clin Obstet Gynecol 1980;23:951–63.
5. Stern RC, Dash R, Bentley RC, Snyder MJ, Haney AF, Robboy SJ. Malignancy in endometriosis: frequency and comparison of ovarian and extraovarian types. Int J Gynecol Pathol 2001;20:133–9.
6. Brinton LA, Gridley G, Persson I, Baron J, Bergqvist A. Cancer risk after a hospital discharge diagnosis of endometriosis. Am J Obstet Gynecol 1997;176:572–9.
7. Obata K, Hoshiai H. Common genetic changes between endometriosis and ovarian cancer [review]. Gynecol Obstet Invest 2000;50 Suppl 1:39–43.
8. Fukunaga M, Nomura K, Ishikawa E, Ushigome S. Ovarian atypical endometriosis: its close association with malignant epithelial tumours. Histopathology 1997;30:249–55.
9. Amemiya S, Sekizawa A, Otsuka J, Tachikawa T, Saito H, Okai T. Malignant transformation of endometriosis and genetic alterations of K-ras and microsatellite instability. Int J Gynaecol Obstet 2004;86:371–6.
10. Nezhat FR, Kalir T. Comparative immunohistochemical studies of endometriosis lesions and endometriotic cysts. Fertil Steril 2002;78:820–4.
11. Martini M, Ciccarone M, Garganese G, et al. Possible involvement of hMLH1, p16(INK4a) and PTEN in the malignant transformation of endometriosis. Int J Cancer 2002;102:398–406.
12. Del Carmen MG, Smith Sehdev AE, Fader AN, et al. Endometriosis-associated ovarian carcinoma: differential expression of vascular endothelial growth factor and estrogen/progesterone receptors. Cancer 2003;98:1658–63.
13. Jiang X, Hitchcock A, Bryan EJ, et al. Microsatellite analysis of endometriosis reveals loss of heterozygosity at candidate ovarian tumor suppressor gene loci. Cancer Res 1996;56:3534–9.
14. Jiang X, Morland SJ, Hitchcock A, Thomas EJ, Campbell IG. Allelotyping of endometriosis with adjacent ovarian carcinoma reveals evidence of a common lineage. Cancer Res 1998;58:1707–12.
15. Dinulescu DM, Ince TA, Quade BJ, Shafer SA, Crowley D, Jacks T. Role of K-ras and Pten in the development of mouse models of endometriosis and endometrioid ovarian cancer. Nat Med 2005;11:63–70.
16. Fenton HJH. Oxidation of tartaric acid in presence of iron. J Chem Soc 1894;65:899–910.
17. Toyokuni S. Iron-induced carcinogenesis: the role of redox regulation. Free Radic Biol Med 1996;20:553–66.
18. Toyokuni S. Iron and carcinogenesis: from Fenton reaction to target genes. Redox Rep 2002;7:189–97.
19. Kuroda H, Mandai M, Konishi I, et al. Human ovarian surface epithelial (OSE) cells express LH/hCG receptors, and hCG inhibits apoptosis of OSE cells via up-regulation of insulin-like growth factor-1. Int J Cancer 2001;91:309–15.
20. Kusakari T, Kariya M, Mandai M, et al. C-erbB-2 or mutant Ha-ras induced malignant transformation of immortalized human ovarian surface epithelial cells *in vitro*. Br J Cancer 2003;89:2293–8.
21. Kyo S, Nakamura M, Kiyono T, et al. Successful immortalization of endometrial glandular cells with normal structural and functional characteristics. Am J Pathol 2003;163:2259–69.
22. Toyokuni S, Okamoto K, Yodoi J, Hiai H. Persistent oxidative stress in cancer. FEBS Lett 1995;358:1–3. Review.
23. Blanc JF, De Ledinghen V, Bernard PH, et al. Increased incidence of HFE C282Y mutations in patients with iron overload and hepatocellular carcinoma developed in non-cirrhotic liver. J Hepatol 2000;32:805–11.
24. Toyokuni S, Tanaka T, Hattori Y, et al. Quantitative immunohistochemical determination of 8-hydroxy-2′-deoxyguanosine by a monoclonal antibody N45.1: its application to ferric nitrilotriacetate-induced renal carcinogenesis model. Lab Invest 1997;76:365–74.

Downloaded from http://aacrjournals.org/clincancerres/article-pdf/14/1/32/1974769/32.pdf by guest on 04 August 2024

25. Lievre V, Becuwe P, Bianchi A, et al. Intracellular generation of free radicals and modifications of detoxifying enzymes in cultured neurons from the developing rat forebrain in response to transient hypoxia. Neuroscience 2001;105:287–97.

26. Nunez MT, Tapia V, Toyokuni S, Okada S. Iron-induced oxidative damage in colon carcinoma (Caco-2) cells. Free Radic Res 2001;34:57–68.

27. Toyokuni S, Uchida K, Okamoto K, Hattori-Nakakuki Y, Hiai H, Stadtman ER. Formation of 4-hydroxy-2-nonenal-modified proteins in the renal proximal tubules of rats treated with a renal carcinogen, ferric nitrilotriacetate. Proc Natl Acad Sci U S A 1994;91:2616–20.

28. Osada Y, Kumagai T, Masuda K, Suzuki T, Kanazawa T. Mutagenicity evaluation of *Schistosoma* spp. extracts by the umu-test and V79/HGPRT gene mutation assay. Parasitol Int 2005;54:29–34.

29. Nelson RL. Dietary iron and colorectal cancer risk [review]. Free Radic Biol Med 1992;12:161–8.

30. Lee DH, Anderson KE, Folsom AR, Jacobs DR, Jr. Heme iron, zinc and upper digestive tract cancer: the Iowa Women's Health Study. Int J Cancer 2005;117:643–7.

31. Stevens RG, Jones DY, Micozzi MS, Taylor PR. Body iron stores and the risk of cancer. N Engl J Med 1988;319:1047–52.

32. Evans AE, D'Angio GJ, Propert K, Anderson J, Hann HW. Prognostic factor in neuroblastoma. Cancer 1987;59:1853–9.

33. Hann HW, Lange B, Stahlhut MW, McGlynn KA. Prognostic importance of serum transferrin and ferritin in childhood Hodgkin's disease. Cancer 1990;66:313–6.

34. Potaznik D, Groshen S, Miller D, Bagin R, Bhalla R, Schwartz M, de Sousa M. Association of serum iron, serum transferrin saturation, and serum ferritin with survival in acute lymphocytic leukemia. Am J Pediatr Hematol Oncol 1987;9:350–5. Erratum in: Am J Pediatr Hematol Oncol 1988 Fall;10:277.

35. Niederau C, Fischer R, Sonnenberg A, Stremmel W, Trampisch HJ, Strohmeyer G. Survival and causes of death in cirrhotic and in noncirrhotic patients with primary hemochromatosis. N Engl J Med 1985;313:1256–62.

36. Bradbear RA, Bain C, Siskind V, et al. Cohort study of internal malignancy in genetic hemochromatosis and other chronic nonalcoholic liver diseases. J Natl Cancer Inst 1985;75:81–4.

37. Hsing AW, McLaughlin JK, Olsen JH, Mellemkjar L, Wacholder S, Fraumeni JF, Jr. Cancer risk following primary hemochromatosis: a population-based cohort study in Denmark. Int J Cancer 1995;60:160–2.

38. Kato J, Kobune M, Nakamura T, et al. Normalization of elevated hepatic 8-hydroxy-2′-deoxyguanosine levels in chronic hepatitis C patients by phlebotomy and low iron diet. Cancer Res 2001;61:8697–702.

39. Richmond HG. Induction of sarcoma in the rat by iron-dextran complex. Br Med J 1959;1:947–9.

40. Okada S, Midorikawa O. Induction of rat renal adenocarcinoma by Fe-nitrilotriacetate (Fe-NTA). Jpn Arch Intern Med 1982;29:485–491. [Japanese]

41. Li JL, Okada S, Hamazaki S, Ebina Y, Midorikawa O. Subacute nephrotoxicity and induction of renal cell carcinoma in mice treated with ferric nitrilotriacetate. Cancer Res 1987;47:1867–9.

42. Okada S, Hamazaki S, Toyokuni S, Midorikawa O. Induction of mesothelioma by intraperitoneal injections of ferric saccharate in male Wistar rats. Br J Cancer 1989;60:708–11.

43. Seril DN, Liao J, Ho KL, Warsi A, Yang CS, Yang GY. Dietary iron supplementation enhances DSS-induced colitis and associated colorectal carcinoma development in mice. Dig Dis Sci 2002;47:1266–78.

44. Van Langendonckt A, Casanas-Roux F, Donnez J. Iron overload in the peritoneal cavity of women with pelvic endometriosis. Fertil Steril 2002;78:712–8.

45. Van Langendonckt A, Casanas-Roux F, Eggermont J, Donnez J. Characterization of iron deposition in endometriotic lesions induced in the nude mouse model. Hum Reprod 2004;19:1265–71.

46. Deugnier Y, Turlin B. Iron and hepatocellular carcinoma [review]. J Gastroenterol Hepatol 2001;16:491–4.

47. Jungst C, Cheng B, Gehrke R, et al. Oxidative damage is increased in human liver tissue adjacent to hepatocellular carcinoma. Hepatology 2004;39:1663–72.

48. Chapoutot C, Esslimani M, Joomaye Z, et al. Liver iron excess in patients with hepatocellular carcinoma developed on viral C cirrhosis. Gut 2000;46:711–4.

49. Turlin B, Juguet F, Moirand R, et al. Increased liver iron stores in patients with hepatocellular carcinoma developed on a noncirrhotic liver. Hepatology 1995;22:446–50.

Downloaded from http://aacrjournals.org/clincancerres/article-pdf/14/1/32/1974769/32.pdf by guest on 04 August 2024